Functional Characterization of an Enzymatically Degradable Multi-Bioactive Elastin-Like Recombinamer

Alessandra Girotti, Juan Gonzalez-Valdivieso, F. Javier Arias, Mercedes Santos*

Laura Martín.

BIOFORGE (Group for Advanced Materials and Nanobiotechnology), CIBER-BBN
University of Valladolid, 47011 Valladolid, Spain

*Corresponding author: Alessandra Girotti

Tel: (+34) 983 186379; Fax: (+34) 983 184 698. E-mail: agirotti@bioforge.uva.es

Abstract

One of the main goals in both tissue engineering and regenerative medicine is to design innovative synthetic scaffolds that can simulate and control the communication pathways between cells and the extracellular matrix (ECM). In this context, we describe herein the characterization of protein polymer, a recombinant elastin-like recombinamer (ELR) designed for developing tissue-engineered devices for use in vascular regeneration. This ELR is composed of an elastin-like backbone that contains a fibronectin domain, which provides specific, endothelial cell adhesion, and a protease target domain directed towards specific proteases involved in ECM remodeling. We

also compare the specific response of endothelial and fibroblast cells to ELR scaffolds and show that cell adhesion and spreading on this ELR is significantly higher for endothelial cells than for fibroblasts. The reactivity of this polymer and its hydrogels to specific enzymatic degradation is demonstrated *in vitro*. As with natural elastin, enzymatic hydrolysis of the ELR produces elastin-derived peptides, or "matrikines", which, in turn, are potentially able to regulate important cell activities.

Keywords

Artificial Extracellular Matrix, Elastin-Like Polymer, Enzymatic Biodegradation.

1. Introduction

Tissue engineering is a therapeutic field which aims to replace and repair a damaged tissue or organ for its functional recover [1]. To attain this purpose, many areas of biomaterials science are currently focused on the search for new advanced materials that can mimic the rich functionality of the proteins found in the natural extracellular matrix (ECM) as a way of achieving a significant breakthrough in the performance provided by the more conventional substrates used in tissue engineering [1-4]. In this sense, these new artificial devices, when placed into a biological environment, should show superior biocompatibility by integrating with the host tissue without eliciting a significant immune response. Likewise, their degradation products should be innocuous, in the sense of being nontoxic, and should not cause inflammation. Optimal physicochemical properties, such as mechanical properties and their intrinsic smart nature, are crucial, whereas other features such as shape, compartmentalization, and surface texture can all improve their functionality still further. An ideal biomaterial should assume the correct surface and internal topography, density, and porosity to create good artificial devices [5, 6]. To mimic the ECM's functionality and its inter-relationship with the cell, the

artificial scaffold must also integrate specific bioactivities that modulate cellular signaling processes in the form of adhesion, migration, differentiation, and proliferation, and provide guidance for new tissue formation or biodegradation [5]. Finally, a tissue engineering scaffold should be biodegradable. Thus, after serving as a temporary scaffold it should ideally degrade into nontoxic products so that second surgery is not required to remove it [7]. Coordinated rates of scaffold degradation and new tissue generation are therefore also essential elements [8].

One of the main strategies for discovering enhanced biomaterials for tissue engineering is to build artificial materials from natural building blocks such as protein-based polymers (PBP) [2]. Biomaterials composed of natural building blocks derived from ECM proteins can offer an excellent opportunity to mimic the properties, intrinsically included in their amino acid sequence, that nature has improved and refined during the course of evolution [6]. Moreover, current advances in genetic engineering and recombinant DNA techniques have afforded us the ability to create almost any DNA duplex codifying any amino acid sequence at will, which means that we can assemble tailored specific protein domains to obtain efficient protein materials [9]. In this sense, PBPs and, more specifically, their recombinant versions, by the very nature of their composition and the way they are produced, share the best properties of both biological and artificial materials. Thus, they can be as complex and functional as natural proteins but with a composition that is fully controlled and is the exclusive result of engineering design.

Elastin-like polymers (ELPs) are some of the most attractive PBP candidates for artificial ECM proteins. ELPs are based on repeat sequences, the so-called elastomeric

domains, found in an ECM protein, namely natural elastin [10, 11]. Furthermore, they retain the latter's mechanical properties, especially its ideal elasticity and outstanding resistance to fatigue [12]. The term Elastin-Like Recombinamer (ELR) has been coined in order to refer ELPs which are obtained by means of genetic engineering and biotechnological methods [13]. These polymers also show unmatched characteristics in terms of biocompatibility, and combine a strong tendency to self-assemble with an acute smart behavior, depending on the polymeric architecture and environmental conditions [10, 14]. Additionally, specific functionalities, such as cell-binding sequences that modulate cell adhesion through integrins and others bioactive functions, can be included in their structure by adding defined peptide domains derived from different ECM or non-ECM proteins [15-17]. Very diverse synthetic materials have been effectively functionalized with different cell-adhesion peptides, the most common of which is the Arg-Gly-Asp (RGD) peptide sequence or larger sequences containing this tripeptide [17-19]. RGD is a powerful and generic cell-binding domain which is recognized by approximately half of all integrin heterodimers present in numerous cell types [20]. While this peptide is highly appropriate for achieving strong but unspecific cell adhesion, other peptides can determine more specific cell-material interactions. The Arg-Glu-Asp-Val (REDV) peptide sequence, for example, which is found within the alternatively spliced CS5 fibronectin domain, is specifically recognized by the integrin $\alpha 1\beta 4$ [21]. This integrin is present in a few cell lines, and only endothelial cells have been found to show selective binding and retention in REDV-coated surfaces even under flow conditions [22].

Selective adhesion and scaffold invasion of endothelial cells is one of the requirements for integration of synthetic devices in the body, in the construction of artificial blood

vessels, or in the endothelization of intravascular devices [19, 23, 24]. Endothelial cell-adhesion and -migration is fundamental in a number of physiological processes and in the colonization of artificial devices [22] as the construction of new tissue or organs requires endothelial cells to invade them to recreate a capillary network for tissue survival. In other example, the formation of a continuous monolayer of endothelial cells allows the thrombogenicity risk in vascular grafts to be minimized [19]. In the search for functionalized, biocompatible, and bioactive surfaces, protein domains such as RGD or REDV peptides were first included in the ELR structure in a complex and laborious chemical synthesis by Urry and co-workers [25]. Our version of an ELR containing the CS5 fibronectin domain also possesses another functional block derived from the human elastin, in this case a recurring hexapeptide derived from the human elastin exon 24-encoded product, Val Gly Val Ala Pro Gly (VGVAPG). This sequence, which is a target for specific proteolytic enzymes (elastases), was introduced to induce enzymatic hydrolysis of the synthetic scaffold via the same physiological pathways as natural elastin during ECM remodeling [26]. Furthermore, the VGVAPG matrikines released upon hydrolysis of elastin by these elastases are bioactive peptides involved in cell regulation, especially the modulation of proliferation, migration, or protease production [27]. The fragments resulting from ECM hydrolysis possess chemotactic and mitogenic activities for multiple cells [28].

The diverse bioactivities of an ELR containing both specific REDV cell-adhesion domains and elastase targets (REDV-ELP) are characterized in this work.

2. Experimental Section

2.1 ELR Expression and Purification.

Standard molecular biology techniques were used to construct two ELR genes (ELR -REDV and ELR -IK). Polymer production was carried out using cellular systems for genetically engineered protein biosynthesis in *Escherichia coli*, while their purification was performed with several cycles of temperature-dependent reversible precipitation, as described elsewhere [13]. The purity and molecular weight of the proteins were verified by SDS-PAGE gels, amino-acid analysis, and mass spectrometry (MALDI-TOF).

2.2 Hydrogel and film manufacture.

Two kind of ELR scaffolds were used in this work: films for *in vitro* cell tests and cylindrical hydrogel disks for enzyme-degradation studies. In both cases, a cross-linking reaction was carried out with hexamethylene diisocyanate (HMDI), a Lys-targeted homobifunctional cross-linker, as described elsewhere [29]. HMDI and the solvents acetone, dimethylformamide (DMF), and dimethyl sulfoxide (DMSO) were purchased from Sigma Aldrich.

ELR films were obtained by solvent casting and subsequent cross-linking. Briefly, 50 mg/mL of aqueous ELR (either REDV-ELR or IK-ELR) solution was deposited on piranha-activated circular cover glasses (diameter: 12 mm; Thermo Scientific) and the samples kept at 60 C for 8 h. The dry films were then cross-linked by immersion in a 10% HMDI/acetone solution overnight. Acetone was used because the ELR s are not soluble in this solvent whereas the cross-linker is. After cross-linking, the film adhered to the cover glass was washed thoroughly with Milli-Q water until complete removal of the solvent and any remaining cross-linker. The films used were sterilized by UV exposure overnight and stored in 70% ethanol. Before use, they were washed with

sterile Milli-Q water and PBS and placed in a 24-well cell-culture plate from Corning Inc. Costar (Costar).

Hydrogel disks were prepared by dissolving the corresponding ELR s and HMDI in 20/80 (v/v) DMF/DMSO solution. The stoichiometric relationship between the HMDI functional group and lysine was 1.25:1 equivalents. The final ELR concentration was 70 mg/mL. The solution was cast in polytetrafluoroethylene molds (diameter: 13.5 mm; thickness: 2 mm) at room temperature, and the cross-linking reaction was stopped after 2 h. This solvent system was chosen because both the ELR s and the cross-linker are soluble in it. The cross-linked hydrogels were exhaustively washed with Milli-Q water to eliminate the solvents and any remaining cross-linker.

2.3 Cell Culture.

Human umbilical vein endothelial cells (HUVECs; cat. no. cc-2517) were grown in endothelial growth medium which was replaced every two days (EGM; Clonetic, cat. no. cc-3124), both were purchased from Lonza (Lonza Walker). Human foreskin fibroblasts HFF-1 (SCRC-1041) were maintained in Dulbecco's modified Eagle's medium (DMEM cat. no. 30-2002) supplemented with 15% fetal bovine serum (FBS, cat. no. 30-2021) purchased from American Type Culture Collection (ATCC, USA) and penicillin 10^4 U/ml-streptomycin 10 mg/ml (Sigma Aldrich cat. no. P4333). Cells were incubated at 37 C in a 5% CO_2 humidified environmental chamber.

Trypan Blue stain 0.4% (Sigma Aldrich, cat. no. T6146), PBS (cat. no. 17-516F), HEPES (cat. no. CC-5024), trypsin-versene EDTA (cat. no. 17-161E), DAPI (cat. no. PA-3013), and Phalloidin-Alexa Fluor488 Conjugate (cat. no. PA-3010) were

purchased from Lonza. The remaining consumables for cell culture were obtained from Corning Inc. Costar.

2.4 Cell-Adhesion Assay.

Near confluence cells (passages 2-7) were harvested mechanically with a cell scraper and subsequently enzymatically processed in a short trypsin-EDTA treatment. They were then washed and resuspended in serum-free culture medium (EBM Clonetics cat. no. cc-3121 for HUVECs and DMEM for fibroblasts), and seeded at 10,000 cells/cm^2 on the sterilized ELR films described above deposited in a 24-well plate. Before seeding, cell counts were evaluated using a standard Trypan Blue exclusion assay. Sixteen hours after cell seeding, the films were washed with PBS to remove nonadhered cells and then fixed.

Fibronectin (20 μg/ml; cat. no. F0895 Sigma Aldrich) and 0.5% bovine serum albumin (cat. no. A1933 Sigma Aldrich) in PBS (positive- and negative-binding controls, respectively) were deposited on circular cover glasses in 24-well cell plates and coated for 16 h at 4 °C. The plates were washed three times with PBS 0.05%/Tween-20 and then blocked for 1 h in 1% BSA at 37 °C.

Samples for phase-contrast, epifluorescence, or differential interference contrast (DIC) microscopy (Nomarski) were fixed in 4% paraformaldehyde for 10 min, permeabilized with 0.2% Triton X-100, and stained with the fluorescent dyes Phalloidin-Alexa Fluor488R or DAPI, as indicated in the text.

Each ELR -type film was tested in triplicate and images from nine randomly selected fields were taken. The cells were counted manually using a Nikon Eclipse Ti inverted microscope (Nikon Instruments/Europe) at a magnification of 10-20-40X. Each assay was repeated three times. The cell number and dimensions were determined using the NIS Elements BR program (version 3.05) and a monochrome camera (model DS-2MBWc).

Films seeded with cells for SEM analysis were fixed in Palay fixative (1% gluteraldehyde and paraformaldehyde in 0.1 N calcium chloride solution) at pH 7.4 for 2 h at room temperature. Samples were progressively dehydrated in ethanol solutions (15%, 30%, 50%, 70%, 90%, and three times 100%) for 20 min each and then transferred to a desiccator for 25 min to avoid water contamination. Finally, they were mounted on stubs and sputter-coated with 10 nm gold.

2.5 Enzymatic digestion of ELR s and hydrogels.

The biodegradability of ELR s and their matrices was investigated using two different proteolytic enzymes: human leukocyte elastase I (EC 3.4.21.37) and pancreatic elastase I (EC 3.4.21.36), both of which were purchased from Sigma Aldrich.

Thus, 250 μg of ELR was incubated with 0.06 units of human leukocyte elastase I at 37 °C in 500 μL of 50 mM sodium phosphate buffer (pH 6). Aliquots were removed at regular intervals and mixed with three volumes of SDS-PAGE loading buffer and frozen. The time course of enzymatic degradations was analyzed in glycine SDS-PAGE and tricine SDS-PAGE gels, both of which were copper-stained.

ELR -derived hydrogels (14 μg of ELR per hydrogel) were incubated with one unit of pancreatic elastase I in 400 μL of 100 mM Tris buffer (pH 8) at 37 °C. The hydrogel degradation rate was assessed by determining the weight loss at set times.

2.6 Statistical analysis.

One-way analysis of variance (ANOVA) was used to evaluate the data with *post hoc* differences between groups using Bonferroni's corrected t-test with GraphPad Prism 4.0. A p-value of less than 0.05 was considered to be statistically significant (indicated in figures with asterisks [*]: * $P < 0.05$; ** $P < 0.01$; *** $P < 0.001$). Error bars represent the standard error of the mean. Each experiment was repeated three times.

3. Results and Discussion

3.1 Design and Synthesis of ELRs

The structure of the ECM is an exquisite example of how functionality can arise from the complex and well-defined primary sequences of its macromolecular constituents. In this work we employed ELR s that mimic some characteristics of the natural protein components of the ECM.

REDV-ELR is an 877 amino-acid complex polymer whose complete sequence is: MESLLP[$(VPGIG)_2$(VPGKG)$(VPGIG)_2$EEIQIGHIPREDVDYHLYP$(VPGIG)_2$(VPGKG)$(VPGIG)_2$$(VGVAPG)_3]_{10}$V. Each monomer contains four different building-blocks. The first one is the elastomeric pentapeptide (VPGIG), which gives the desired mechanical and biocompatibility behavior. The second building block is a variation of the first with a lysine substituting the isoleucine so that the lysine's free γ-amino group

can be used for cross-linking. The third domain is the CS5 domain of natural fibronectin, which contains the well-known REDV, a cell-selective adhesion peptide which is specifically recognized by the integrin $\alpha 1\beta 4$ [30]. This integrin is found in a few cell lines and, overall, is preferentially expressed in endothelial cells [22]. Finally, the fourth block in the monomer contains the human elastin hexapeptide VGVAPG sequence. This hexapeptide is a target for the elastases that rearrange and renovate the extracellular matrix. It was introduced as a way of driving the polymer's bio-processability and its reabsorption and to play a further role in tissue repair. This hexapeptide is the receptor binding site on the molecule [28] and, when released upon partial hydrolysis of elastin, is able to regulate cell activities and to stimulate the matrix metalloproteinases MMP-2 and MMP-1 [31, 32].

The control ELR (IK-ELR) is exclusively composed of the structural elements of the former, i.e. the pentapeptides VPGIG and VPGKG, with the same arrangement; its complete sequence is MESLLP$[(VPGIG)_2(VPGKG)(VPGIG)_2]_{24}$V. This polymer was designed as a negative control in the cell-culture experiments and elastase assays. IK-ELP lacks bioactive domains but shows all the mechanical and cross-linking properties of its related REDV-ELR. The two ELR s were bioproduced in *Escherichia coli* and purified by several cycles of temperature-driven reversible precipitations. The SDS-PAGE, amino acid composition analysis, and MALDI-TOF spectra showed that the two ELR s were pure and that their composition and molecular mass matched the expected results (data not shown).

3.2 Characterization of ELR scaffolds.

ELR scaffolds were produced in order to see whether the ELR s showed the desired effect on cell culture, in accordance with their sequence design. The approach of developing polymer scaffolds in the form of consistent films by chemical cross-linking of solvent-cast materials is a simpler method of creating appropriate scaffolds. This kind of support facilitates the visualization and analysis of cell cultures whilst preserving all their functional and structural properties. The macroscopic characteristics of ELR - based hydrogels and films were found to be similar as we obtained solid, consistent, transparent, insoluble swell scaffolds in all cases. The films' microscopic structure showed a relatively flat surface interrupted where the pellicle folds itself and is raised up to form ribbon-like structures (Fig. 1, Fig. 2 E, F, G and H, Fig. 3), and the SEM analysis showed a similar microporous spacing (Fig. 1). The cross-sectional view (Fig. 1 A) shows a compact polymer layer with a thickness of 5-6 μm totally covering the glass substrate.

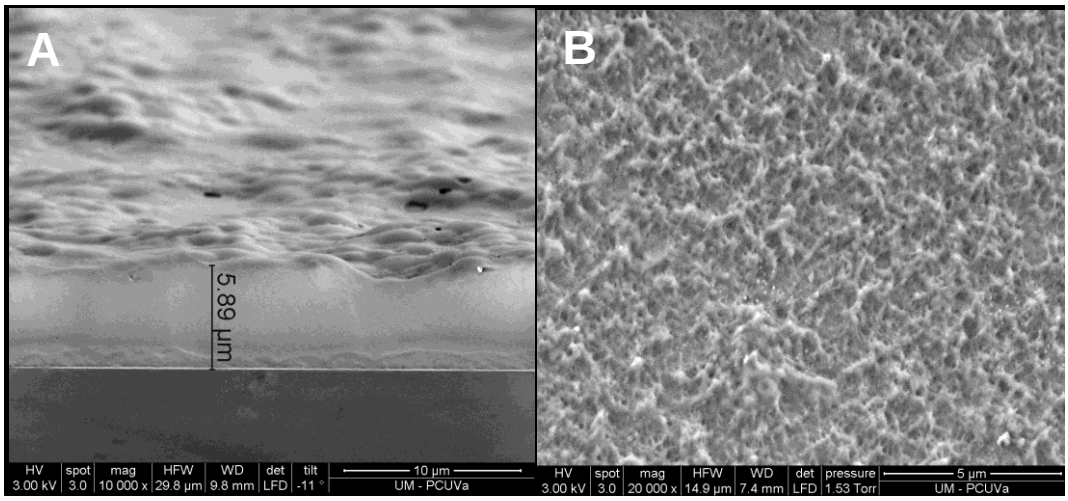

Figure 1. SEM images of REDV-ELP cross-linked films used in cellular "*in vitro*" studies: cross-sectional (A) and surface (B) views.

3.3 Cell adhesion of HUVEC to ELR films.

With the aim of evaluating the response of cells when deposited on ELR scaffolds with different bioactivities, *in vitro* studies of their adhesion and morphology were performed using both HUVEC endothelial and HFF1 fibroblast cells. The complete adhesion of endothelial cells was achieved upon extending the incubation time for a further 16 hours [10]. We used basal medium (EBM) for the first six hours to avoid interference from serum compounds and complements in the specific adhesion mechanism , then replaced this with complete EGM medium to avoid any damage to the physiological cell process and thus allow a longer incubation time. Finally, the cells were fixed and stained to show their inner cellular structure, cytoskeleton, and nuclei. HUVEC cells cultured on REDV-ELP scaffolds showed a well-spread morphology with large extensions and numerous pseudopodia, and their cytoskeleton actin filaments (green stained) were well organized in stress fibers, thereby indicating a strong adhesion (Fig. 2 A, C and E). Previous studies have shown that the forces associated with maximal adhesion and spreading appear to be localized at the tips of the pseudopodia and that an increase in adhesion traction force results in an increase in cell area [33]. In our case, the irregular shape of the surface (Fig. 2 E) does not affect the active spread of the cells but also appears to induce the formation of focal adhesions on the promontories.

In contrast, the cell number and morphology of HUVECs seeded on IK-ELP, the negative control scaffold that lacks bioactive sequences, were clearly different to those observed with the REDV-ELP scaffold (Fig. 2 B and D). Thus, only a few rounded cells were found with no obvious focal attachments to the surface (Fig. 2 F). In addition, these cells showed a smaller area with minor or inexistent lamellipodial extensions, thereby suggesting that minor passive adhesion is the main cell-scaffold interaction.

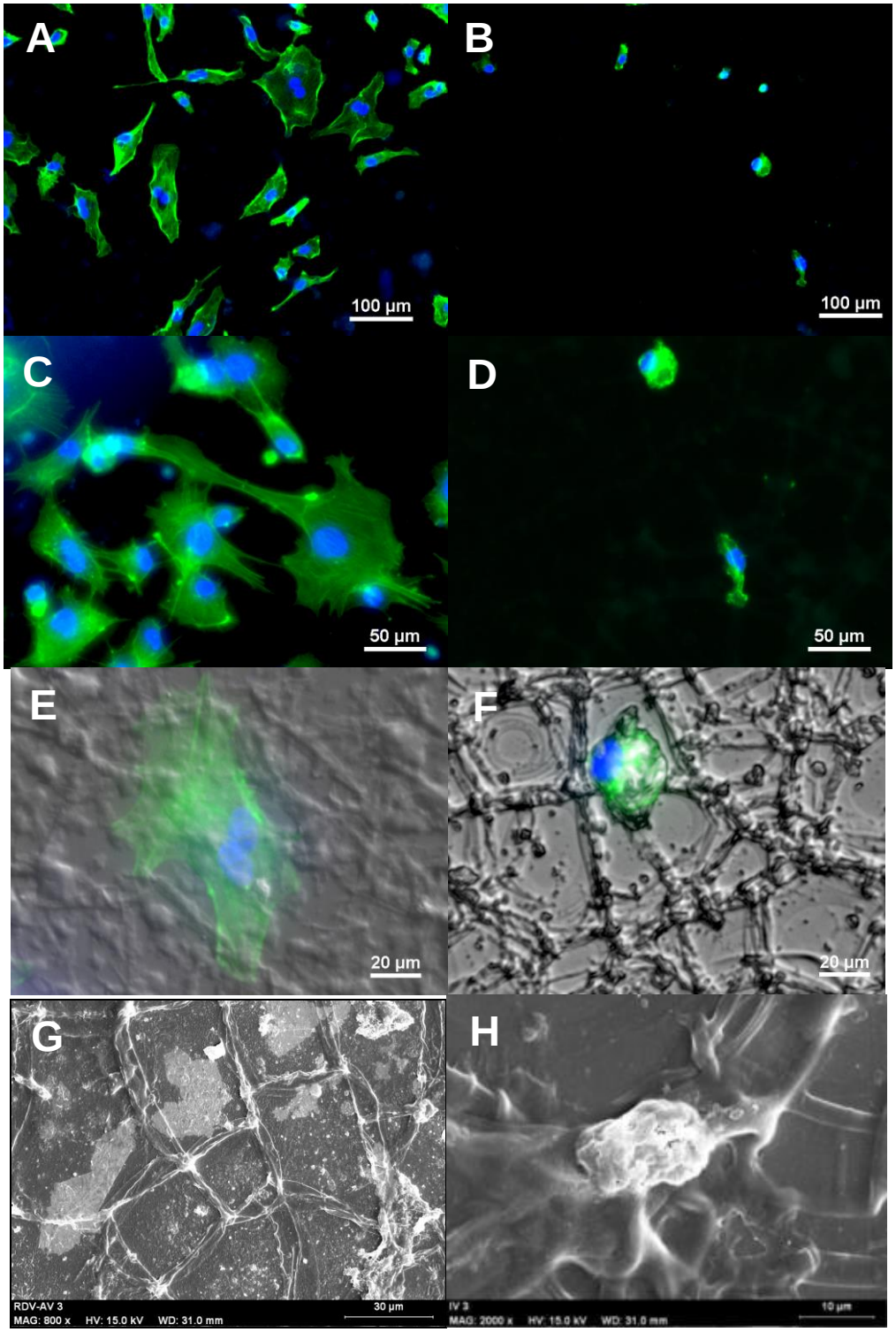

Figure 2. Representative microscopy images of HUVECs seeded on ELR films after 16 hours of incubation. A and B (10x), C and D (20x): Phalloidin Alexa Fluor488 and DAPI staining. E and F: Phalloidin Alexa Fluor488 and DAPI staining with Nomarski images (40x). G and H: Scanning electron micrographs. A, E, C and G: cells seeded on REDV-ELP films. B, D, F and H: cells seeded on IK-ELP films.

Similar results were found in the SEM analysis. The flattened HUVEC cells, which possess an almost two-dimensional structure, were almost indistinguishable from the REDV-ELP substrate (Fig. 2 G) and were significantly larger than those seeded on IK-ELP scaffolds, where the globular cell showed adhesion without spreading (Fig. 2 H).

3.4 Cell adhesion of fibroblasts to ELR films.

To test the specificity of these REDV-containing scaffolds towards endothelial cells, a new set of *in vitro* tests was performed using fibroblasts. In general, fibroblasts have been reported to be one of the most adherent cell types for a wide range of surfaces, irrespective of their hydrophobicity/hydrophilicity and the existence of cell-adhesion domains on their surface [34]. A comparison with the adhesion of HUVECs to the two scaffolds used herein could therefore be considered a test of the actual capacity of the REDV-ELP to promote the selective adhesion of endothelial cells. In this case, the morphology of the fibroblasts seeded on REDV-ELP and IK-ELP is quite similar (Fig. 3 A, B, C and D). A large number of total cells adhere to both films but show a nonspread globular shape completely different from fibroblasts seeded on fibronectin (Fig. 3 E) or polystyrene (data not shown), two standard cell supports in which fibroblasts have shown excellent adhesion capabilities. The fibroblast morphology on ELR films was similar to that of cells seeded on BSA (Fig. 3 F) or polyethylene glycol (data not shown) layers, both of which are well-known for their anti-fouling properties [35].

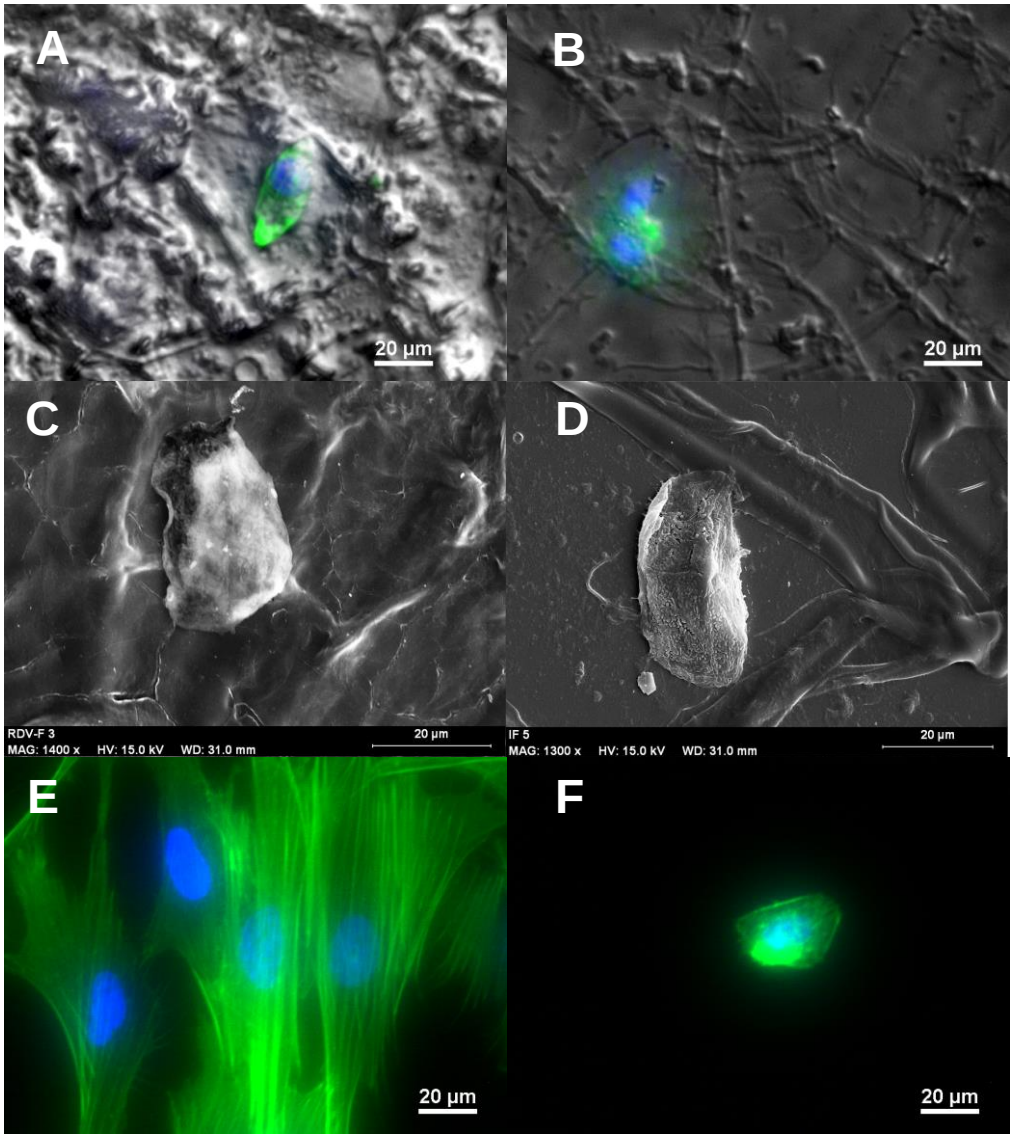

Figure 3. Microscopy images of HFF 1 fibroblasts seeded on ELR films after 16 hours of incubation. A and B: Phalloidin Alexa Fluor488 and DAPI staining with Nomarski images (40x). C and D: Scanning electron micrographs; E and F: Phalloidin Alexa Fluor488 and DAPI staining (40x). A and C: cells seeded on REDV-ELP films. C and D: cells seeded on IK-ELP films; E and F: cells seeded on fibronectin and BSA, respectively. Scale bars: 20 µm.

A qualitative comparison of endothelial cell adhesion on ELR films with different bioactivities revealed that cells spread better and their area increases in the presence of the adhesion domain.

3.5 Cell spreading on ELR films.

Quantitative experiments confirmed the previous qualitative results. Thus, the interaction between the cells and ELR surfaces was analyzed by cell number quantification of the two cell types. Cell spreading was determined by mean cell area measurements (Fig. 4). HUVEC adhesion to the different ELR scaffolds was found to be dependent on the REDV peptide presence, with the total number of cells on the REDV-ELP being around threefold higher than the total number of cells found on the control sequence (IK-ELP). The high statistical significance of this result confirms the specific effect of this adhesion peptide on HUVEC. This positive effect was not apparent, however, when seeding fibroblasts: these cells showed a significant reduction in the number of cells adhered to REDV-ELP in comparison to IK-ELP. In addition, the difference between the numbers of HUVEC and HFF1 cells indicates that this material clearly benefits the adhesion of endothelial cells over fibroblasts, thus pointing to an important role of the REDV sequence in their discrimination. In general, both ELR scaffolds seeded with fibroblasts showed lower cell numbers than with HUVEC on REDV-ELP, thus showing that this kind of surface does not stimulate fibroblast colonization. Despite the presence of the bioactive sequence, REDV-ELP does not determine a positive interaction, either specific or nonspecific, with the films. On the contrary, we found a significantly lower number of fibroblasts on REDV-ELP films than on IK-ELP ones (see Fig. 4).

Previous studies have shown that hydrophobic surfaces can enhance passive or nonspecific adhesion due to the more efficient exposure of the hydrophilic bioactive domains of fibronectin or serum proteins [34]. According to the results described herein, and despite the relatively hydrophobic composition of the polymers used, however, this effect does not appear to be significant in our systems. This selective antifouling property will be tested in future studies with other cell types to determine its potential non-thrombogenicity in light of increasing interest in the use of this biomaterial for vascular grafts and other applications.

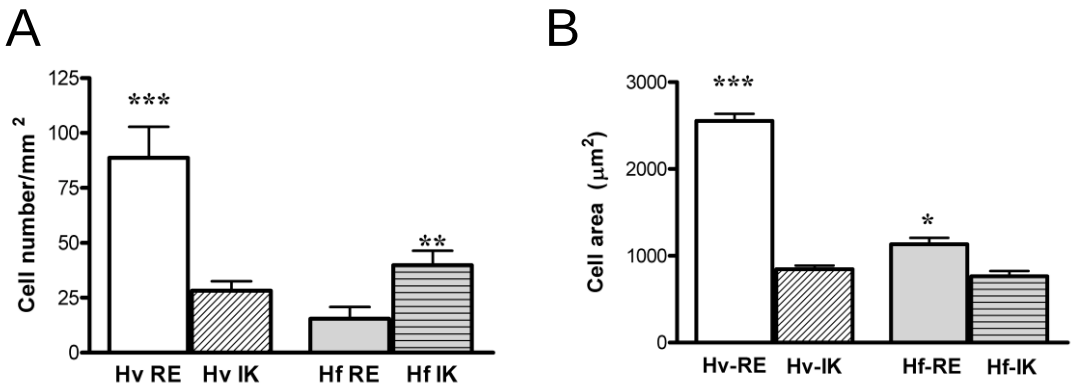

Figure 4 : Comparison of endothelial HUVEC (Hv) and fibroblast HFF1 (Hf) adhesion and morphology on bioactive REDV-ELP (RE) and negative control IK-ELP (IK) after 16 hours of seeding. Panel A: samples are represented as the average cell number normalized with respect to field area. Panel B: representation of average cell areas. Error bars represent the standard error of the mean. Statistical differences were considered significant at $p < 0.05$.

The studies on cell area show a clear difference between the growth of endothelial cells on ELR s (Fig. 4 B). Thus, HUVECs seeded on REDV-ELP films present a threefold larger mean area than on IK-ELP films, thereby showing that the cells adhere and spread specifically in the presence of the REDV sequence. In contrast, fibroblasts did

not expand over either of the ELR surfaces, thus confirming their anti-adherent properties for this cell type. These results clearly differ from the positive control results found for HFF1 cells seeded on tissue culture polystyrene (2500 μm^2) and fibronectin (2600 μm^2).

3.6 Enzymatic degradation of ELRs.

To test the biodegradability of the REDV- ELR scaffold via natural ECM remodeling routes, a matrix protease-sensitive assay was performed on both soluble polymer and polymer-derived hydrogels using two different serine protease elastase enzymes (EC 3.4.21.36 and 3.4.21.37). REDV-ELP biopolymer biodegradation was tested with human leukocite elastase I, which has already been shown to recognizes the target sequence and digest the peptide bound to the major (Val-Ala) and minor (Gly-Val) cleavage sites in the hexapeptide Val-Gly-Val-Ala-Pro-Gly [26].

When the noncross-linked ELRs were incubated under optimal enzymatic conditions, the elastases quickly and exhaustively digested the REDV biopolymer. Digestion was already obvious after the first minute (lane 1), and after 40 minutes no intermediate digestion products were visible (Fig. 5A, lane 40), although neither were the total digestion products, which may be contained in the SDS gel front. IK-ELP was used as the control since this polymer does not have the VGVAPG hexapeptide. No significant specific or nonspecific degradation of IK-ELP was observed, even after extension of the digestion time up to 19 hours (Fig. 5A, lanes 0 and 1140). Tricine SDS-PAGE[39] was used to further separate and analyze the products resulting from the complete digestion of REDV-ELP. This electrophoresis technique allows minor bands corresponding to peptides with a molecular weight lower than 9000 Da to be resolved. A theoretical study

of elastase activity on REDV-ELP predicted the production of numerous proteolytic peptides (more than sixty). The size of the final products in a complete digestion was predicted to range from 200 to 9000 Da, with the majority of fragments being found around 7000-7500 Da. The bands for ELR proteolytic fragments resulting from a complete enzymatic hydrolysis, as resolved by SDS-PAGE, showed a molecular weight corresponding to that of the theoretical fragments produced by specific elastase proteolysis (Fig. 5 B).

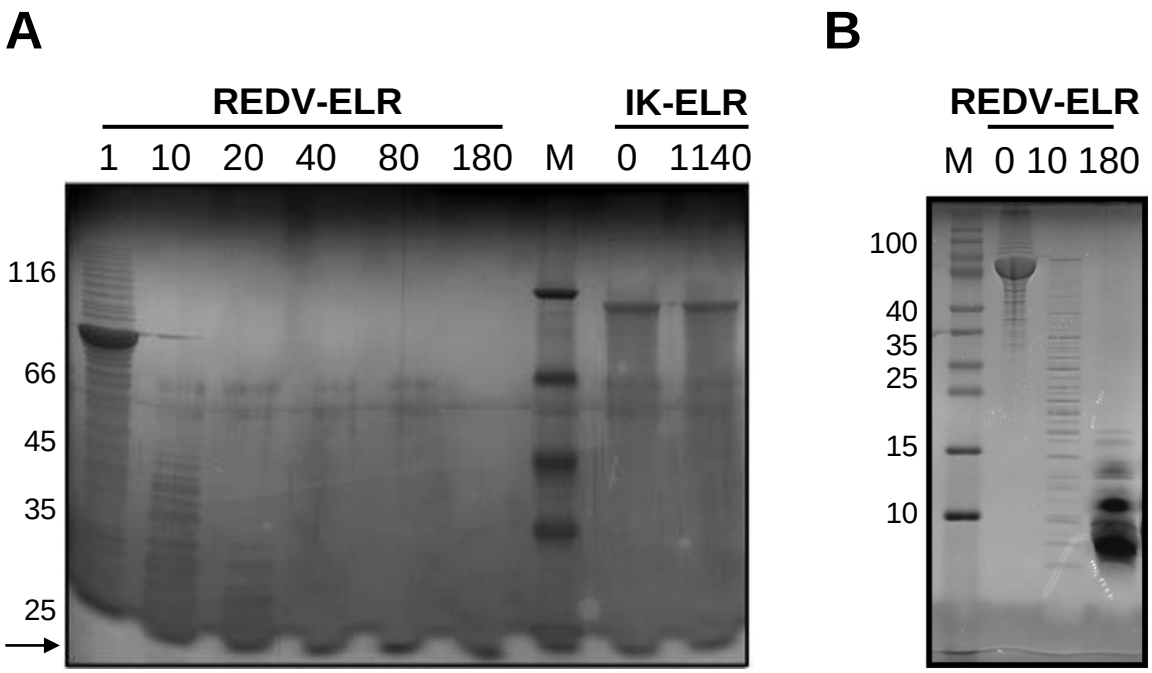

Figure 5. SDS-PAGE analysis of the ELR proteolysis of recombinant biopolymers showing the digested fragments obtained at different incubation times (in minutes) at 37 °C. Panel A: Glycine SDS-PAGE (12%) showing the lanes for REDV- ELR (samples from 1 minute to 3 hours) and IK- ELR (negative control; 0 and 19 hours). Panel B: Tricine SDS-PAGE (16%) separation of partial lane 10 and total digestion fragments of REDV- ELR lane 180. The numbers above the lanes refer to the incubation times in

minutes. The position and size (kDa) of molecular weight protein markers are indicated with numbers at the side of the images, whereas the arrow indicates the SDS gel front.

3.7 Enzymatic degradation of the bioactive scaffolds.

Pancreatic elastase I was used for hydrogel degradation studies. Both enzymes are serine proteases with analogous substrate specificities and similar tertiary structures, especially in their active-site regions [36], although the latter is more stable than the human leukocyte elastase used above, which facilitates the study of matrix enzymatic digestion over longer periods of time. Similar results were found for the enzymatic hydrolysis of REDV- ELR -derived hydrogels and the proteolysis of noncross-linked ELRs (result not shown). The enzyme-sensitivity of the ELR biopolymers and their resulting scaffolds was found to be strictly correlated with the presence of the specific elastase target sequences. Thus, enzymatic proteolysis caused a rapid weight loss of the hydrogels in the presence of one unit of elastase for the REDV- ELR -derived scaffolds, with the hydrogels having disappeared completely after 7 hours of incubation at 37 °C (see Fig. 6). No enzymatic activity was detectable for hydrogels made from the control IK- ELR. These control hydrogels did not degrade and their weight remained constant during the whole experiment (248 h; Fig. 5).

The presence of the repeated minor cleavage site (Gly-Val) in the backbone of both ELR s appears to have no influence on elastase activity; in fact, no observable effects of proteolysis or poorly efficient degradations were observed with either the biopolymer or the control matrices. The chemical modifications introduced upon cross-linking did not alter the elastase sensitivity of the ELR s, and only the expected dependence of the degradation kinetics on the degree of cross-linking was observed, with a slower

degradation rate being found for higher degrees of cross-linking (result not shown). This effect is likely governed by the diffusion rate of elastase into the hydrogel network.

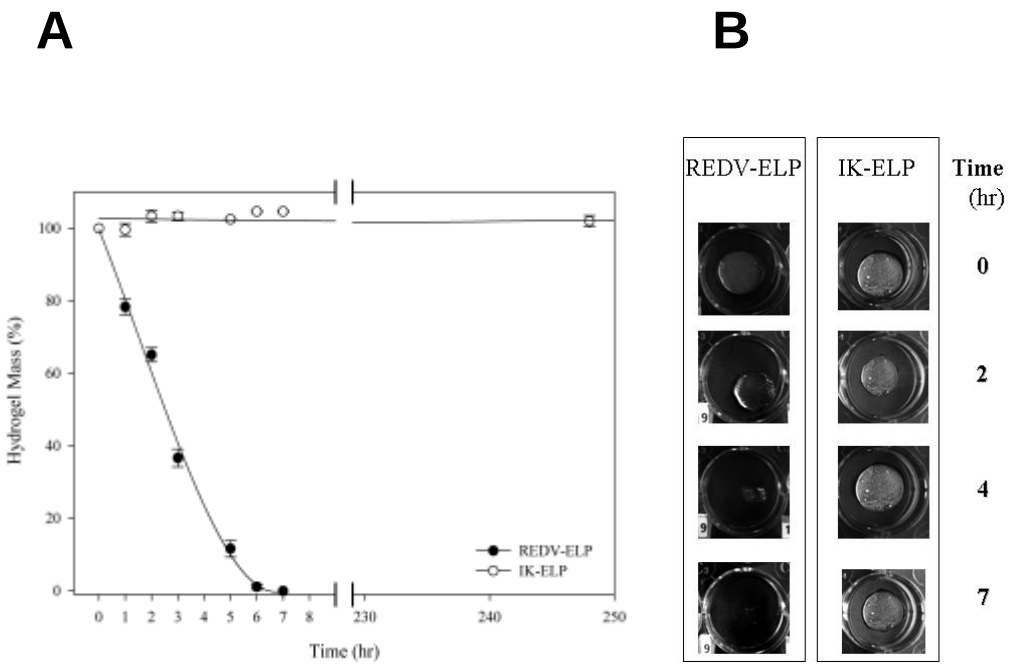

Figure 6. Enzymatic digestion of the ELR hydrogels was assessed by measuring the weight loss upon proteolysis. Panel A: Degradation kinetics of ELR hydrogels with (REDV- ELR) or without (IK- ELR) the elastase target sequence. Data represent the mean weight of normalized hydrogels as a percentage of total weight at time 0. Panel B: Macroscopic observation of enzymatic erosion of cross-linked ELR hydrogels.

4. Conclusions

We have studied the biofunctionality of ELR -based multifunctional biomaterials which have been designed to show improved endothelial cell adhesion and function. The REDV- ELR material is formed from ECM structural protein domains that confer the expected and well-studied elastic and biocompatible properties along with endothelial cell adhesion and bioprocessability upon specific enzymatic digestion. A comparison of the cell behavior between controls and REDV- ELR films has shown that our REDV material promotes specific cell attachment via integrin receptors, specifically $\alpha_4\beta_1$,

expressed in endothelial cells. In fact, HUVEC cultures showed highly significant differences in terms of cell number, adhesion, spreading, and morphology depending on the ELR scaffolds used. The culture of fibroblasts on ELR films has shown that REDV-ELR is a selective scaffold which does not promote HFF1 adhesion and that the morphology of HFF1 cells is similar on REDV- ELR and IK- ELR control scaffolds, despite the latter having no bioactivity, but completely different to that found for fibronectin on cell-culture grade polystyrene.

The insertion of a protease recognition site for human elastases has allowed us to achieve complete degradation of the biopolymer in the same way as natural elastin during the ECM rearrangement. These findings were the same for both melt noncross-linked REDV-ELP and its cross-linked hydrogels, and, in both cases, were protease target domain dependent. The chemical modifications introduced upon cross-linking do not alter the elastase sensitivity of rELPs significantly. Partial degradation of the REDV-ELP materials generates fragments whose sequences are identical to the protein fragments comprising the ECM. Some of these degradation products of natural or REDV-ELP scaffolds could be implicated in natural cell-matrix communication channels, cell regulation, and in the modulation of tissue remodeling. The erosion or complete degradation of the scaffold determines the exclusive release of small peptides and amino acids.

REDV-ELP scaffolds have therefore demonstrated their ability to undergo enzymatic remodeling, whereas most other synthetic scaffolds degrade by simple, non-cell-assisted hydrolysis. This cell-mediated process proceeds with a complex physiological control that is not possible in purely hydrolytic systems, therefore the inclusion of this kind of

bioactive motif in the rELP allows the creation of more complex and sophisticated tissue-engineering systems with specific cell-adhesion bioactivity and target sequences for enzymes involved in the native tissue-remodeling process.

Acknowledgments

The authors are grateful for the funding from the European Commission (NMP-2014-646075), the Spanish Government (PCIN-2015-010 (FunBioPlas), MAT2015-68901-R, MAT2016-78903-R, MAT2016-79435-R), Junta de Castilla y León (VA317P18) and Centro en Red de Medicina Regenerativa y Terapia Celular de Castilla y León.

Conflict of interest

The authors declare no competing financial interest.

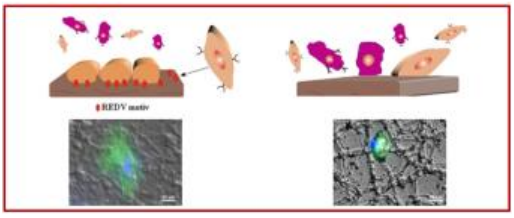

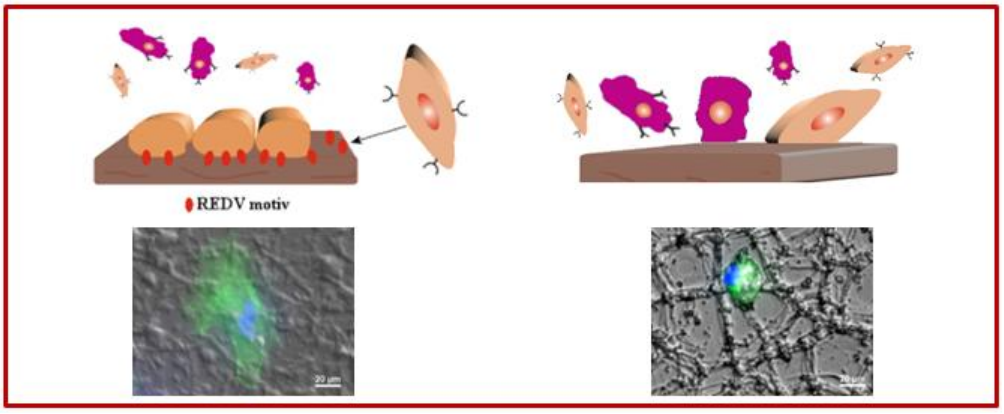

References

[1] R. Langer, J. Vacanti, Advances in tissue engineering, J Pediatr Surg. 51 (2016) 8-12. https://doi.org/10.1016/j.jpedsurg.2015.10.022
[2] D. Nettles, A. Chilkoti, L. Setton, Applications of elastin-like polypeptides in tissue engineering, Adv Drug Deliv Rev. 62 (2010) 1479-1485. https://doi.org/10.1016/j.addr.2010.04.002
[3] M.C. Koetting, J.T. Peters, S.D. Steichen, N.A. Peppas, Stimulus-responsive hydrogels: Theory, modern advances, and applications, Materials Science and Engineering: R: Reports. 93 (2015) 1-49. https://doi.org/http://dx.doi.org/10.1016/j.mser.2015.04.001
[4] Y. Wu, C. Yu, M. Xing, L. Wang, G. Guan, Surface modification of polyvinyl alcohol (PVA)/polyacrylamide (PAAm) hydrogels with polydopamine and REDV for improved applicability, J Biomed Mater Res B Appl Biomater. 1 (2019) https://doi.org/10.1002/jbm.b.34371
[5] B. Slaughter, S. Khurshid, O. Fisher, A. Khademhosseini, N. Peppas, Hydrogels in regenerative medicine, Advanced materials (Deerfield Beach, Fla.). 21 (2009) 3307-3329. https://doi.org/10.1002/adma.200802106
[6] A. Girotti, D. Orbanic, A. Ibanez-Fonseca, C. Gonzalez-Obeso, J.C. Rodriguez-Cabello, Recombinant Technology in the Development of Materials and Systems for Soft-Tissue Repair, Adv Healthc Mater. 16 (2015) https://doi.org/10.1002/adhm.201500152
[7] I. Manavitehrani, A. Fathi, Y. Wang, P.K. Maitz, F. Mirmohseni, T.L. Cheng, L. Peacock, D.G. Little, A. Schindeler, F. Dehghani, Fabrication of a Biodegradable Implant with Tunable Characteristics for Bone Implant Applications, Bioamcromolecules. 18 (2017) 1736-1746. https://doi.org/10.1021/acs.biomac.7b00078
[8] L. Zhang, X. Liu, G. Li, P. Wang, Y. Yang, Tailoring degradation rates of silk fibroin scaffolds for tissue engineering, J Biomed Mater Res A. 107 (2019) 104-113. https://doi.org/10.1002/jbm.a.36537
[9] J.C. Rodriguez-Cabello, M.J. Pina, A. Ibanez-Fonseca, A. Fernandez-Colino, F.J. Arias, Nanotechnological Approaches to Therapeutic Delivery Using Elastin-Like Recombinamers, Bioconjug Chem. 26 (2015) 1252-1265. https://doi.org/10.1021/acs.bioconjchem.5b00183
[10] D.W. Urry. What sustains life? Consilient mechanisms for protein-based machines and materials. New York: Springer-Verlag; 2006.
[11] M. Santos, S. Serrano-Ducar, J. Gonzalez-Valdivieso, R. Vallejo, A. Girotti, P. Cuadrado, F.J. Arias, Genetically Engineered Elastin-based Biomaterials for Biomedical Applications, Curr Med Chem. (2018) https://doi.org/10.2174/0929867325666180508094637
[12] J.C. Rodriguez-Cabello, I. Gonzalez de Torre, A. Ibanez-Fonseca, M. Alonso, Bioactive scaffolds based on elastin-like materials for wound healing, Adv Drug Deliv Rev. 129 (2018) 118-133. https://doi.org/10.1016/j.addr.2018.03.003
[13] J.C. Rodriguez-Cabello, A. Girotti, A. Ribeiro, F.J. Arias, Synthesis of genetically engineered protein polymers (recombinamers) as an example of advanced self-assembled smart materials, Methods in molecular biology (Clifton, N.J.). 811 (2012) 17-38. https://doi.org/10.1007/978-1-61779-388-2_2
[14] S. Roberts, T.S. Harmon, J.L. Schaal, V. Miao, K.J. Li, A. Hunt, Author Correction: Injectable tissue integrating networks from recombinant polypeptides with tunable order, Nat. Mater. 17 (2018) 1164. https://doi.org/10.1038/s41563-018-0233-z

[15] C. Kilic, A. Girotti, C. Rodriguez-Cabello, V. Hasirci, A collagen-based corneal stroma substitute with micro-designed architecture, Biomaterials Science. 2 (2014) 318-329. https://doi.org/10.1039/c3bm60194c
[16] T. Flora, I.G. de Torre, M. Alonso, J.C. Rodriguez-Cabello, Tethering QK peptide to enhance angiogenesis in elastin-like recombinamer (ELR) hydrogels, J Mater Sci Mater Med. 30 (2019) 30. https://doi.org/10.1007/s10856-019-6232-z
[17] T. Flora, I. Gonzalez de Torre, M. Alonso, J.C. Rodriguez-Cabello, Use of proteolytic sequences with different cleavage kinetics as a way to generate hydrogels with preprogrammed cell-infiltration patterns imparted over their given 3D spatial structure, Biofabrication. 11 (2019) 035008. https://doi.org/10.1088/1758-5090/ab10a5
[18] E. Ruoslahti, RGD and other recognition sequences for integrins, Annual Review of Cell and Developmental Biology. 12 (1996) 697-715.
[19] I.G. de Torre, F. Wolf, M. Santos, L. Rongen, M. Alonso, S. Jockenhoevel, J.C. Rodriguez-Cabello, P. Mela, Elastin-like recombinamer-covered stents: Towards a fully biocompatible and non-thrombogenic device for cardiovascular diseases, Acta Biomater. 12 (2015) 146-155. https://doi.org/10.1016/j.actbio.2014.10.029
[20] R.O. Hynes, Integrins: Bidirectional, allosteric signaling machines, Cell. 110 (2002) 673-687.
[21] J. Liu, S. Heilshorn, D. Tirrell, Comparative cell response to artificial extracellular matrix proteins containing the RGD and CS5 cell-binding domains, Biomacromolecules. 5 (2004) 497-504. https://doi.org/10.1021/bm034340z
[22] S.P. Massia, J.A. Hubbell, Vascular Endothelial-Cell Adhesion and Spreading Promoted by the Peptide Redv of the Iiics Region of Plasma Fibronectin Is Mediated by Integrin Alpha-4-Beta-1, Journal of Biological Chemistry. 267 (1992) 14019-14026.
[23] X. Ding, W. Chin, C.N. Lee, J.L. Hedrick, Y.Y. Yang, Peptide-Functionalized Polyurethane Coatings Prepared via Grafting-To Strategy to Selectively Promote Endothelialization, Adv Healthc Mater. 7 (2018) https://doi.org/10.1002/adhm.201700944
[24] D. Yao, Z. Qian, J. Zhou, G. Peng, G. Zhou, H. Liu, Y. Fan, Facile incorporation of REDV into porous silk fibroin scaffolds for enhancing vascularization of thick tissues, Mater Sci Eng C Mater Biol Appl. 93 (2018) 96-105. https://doi.org/10.1016/j.msec.2018.07.062
[25] A. Nicol, D.C. Gowda, D.W. Urry, Cell adhesion and growth on synthetic elastomeric matrices containing Arg-Gly-Asp-Ser-3, J Biomed Mater Res. 26 (1992) 393-413. https://doi.org/10.1002/jbm.820260309
[26] C. Lombard, L. Arzel, D. Bouchu, J. Wallach, J. Saulnier, Human leukocyte elastase hydrolysis of peptides derived from human elastin exon 24, Biochimie. 88 (2006) 1915-1921.
[27] B. Shokouhi, C. Coban, V. Hasirci, E. Aydin, A. Dhanasingh, N. Shi, S. Koyama, S. Akira, M. Zenke, A.S. Sechi, The role of multiple toll-like receptor signalling cascades on interactions between biomedical polymers and dendritic cells, Biomaterials. 31 (2010) 5759-5771. https://doi.org/10.1016/j.biomaterials.2010.04.015
[28] U.R. Rodgers, A.S. Weiss, Cellular interactions with elastin, Pathologie Biologie. 53 (2005) 390-398.
[29] P.J. Nowatzki, D.A. Tirrell, Physical properties of artificial extracellular matrix protein films prepared by isocyanate crosslinking, Biomaterials. 25 (2004) 1261-1267.
[30] S.C. Heilshorn, K.A. DiZio, E.R. Welsh, D.A. Tirrell, Endothelial cell adhesion to the fibronectin CS5 domain in artificial extracellular matrix proteins, Biomaterials. 24 (2003) 4245-4252.

[31] C. Kawecki, N. Hezard, O. Bocquet, G. Poitevin, F. Rabenoelina, A. Kauskot, L. Duca, S. Blaise, B. Romier, L. Martiny, P. Nguyen, L. Debelle, P. Maurice, Elastin-derived peptides are new regulators of thrombosis, Arterioscler Thromb Vasc Biol. 34 (2014) 2570-2578. https://doi.org/10.1161/atvbaha.114.304432
[32] L. Duca, S. Blaise, B. Romier, M. Laffargue, S. Gayral, H. El Btaouri, C. Kawecki, A. Guillot, L. Martiny, L. Debelle, P. Maurice, Matrix ageing and vascular impacts: focus on elastin fragmentation, Cardiovasc Res. 110 (2016) 298-308. https://doi.org/10.1093/cvr/cvw061
[33] S.P. Carey, K.E. Martin, C.A. Reinhart-King, Three-dimensional collagen matrix induces a mechanosensitive invasive epithelial phenotype, Sci Rep. 7 (2017) 42088. https://doi.org/10.1038/srep42088
[34] A.J. Campillo-Fernandez, R.E. Unger, K. Peters, S. Halstenberg, M. Santos, M.S. Sanchez, J.M. Duenas, M.M. Pradas, J.L. Ribelles, C.J. Kirkpatrick, Analysis of the Biological Response of Endothelial and Fibroblast Cells Cultured on Synthetic Scaffolds with Various Hydrophilic/Hydrophobic Ratios: Influence of Fibronectin Adsorption and Conformation, Tissue Eng Part A. (2008) https://doi.org/10.1089/ten.tea.2008.0146
[35] J.H. Cho, K. Shanmuganathan, C.J. Ellison, Bioinspired catecholic copolymers for antifouling surface coatings, ACS Appl Mater Interfaces. 5 (2013) 3794-3802. https://doi.org/10.1021/am400455p
[36] W. Bode, E. Meyer, J.C. Powers, Human-Leukocyte and Porcine Pancreatic Elastase - X-Ray Crystal-Structures, Mechanism, Substarte-Specificity, and Mechanism-Based Inhibitors, Biochemistry. 28 (1989) 1951-1963.